Received: 2 February 2022 | Revised: 28 February 2022 | Accepted: 21 March 2022

DOI: 10.1002/bio.4237

RESEARCH ARTICLE

LUMINESCENCE WILEY
The Journal of Biological and Chemical Luminescence

A facile fluorescence turn-on biosensor customized for monitoring of protein kinase activity based on carboxylic carbon nanoparticle–peptide complexes

Tingting Feng[1,2] | Shuzhu Yan[2] | Zheng Wang[1] | Xiaohui Fan[1]

[1]Pharmaceutical Informatics Institute, College of Pharmaceutical Sciences, Zhejiang University, Hangzhou, China

[2]College of Traditional Chinese Medicine and Food Engineering, Shanxi University of Chinese Medicine, Jinzhong, China

Correspondence
Tingting Feng and Xiaohui Fan, Pharmaceutical Informatics Institute, College of Pharmaceutical Sciences, Zhejiang University. Hangzhou 310058, China.
Email: tingtingfeng1985@126.com and fanxh@zju.edu.cn

Funding information
Project funded by China Postdoctoral Science Foundation, Grant/Award Number: 2019 M662089; the Science and Technology Innovation Project of Colleges and Universities in Shanxi Province, Grant/Award Number: 2020L0413; National Natural Science Foundation of China, Grant/Award Number: 82003925

Abstract

In this study, we present a facile and low-cost approach for detecting protein kinase A (PKA) by assembling a purpose-designed carboxyfluorescein (FAM)-labelled peptide with carboxylic carbon nanoparticles (CNPs). Fluorescence of the FAM-labelled peptide gradually decreases to a low background signal as a result of the electron transfer from CNPs to FAM-labelled peptide via the peptide, which acts as a bridge. The reaction in the sensor in the presence of adenosine 5′-triphosphate and PKA phosphorylates the substrate peptide and disrupts the electrostatic repulsive force between the CNPs and the peptide, therefore altering the spectroscopic signal of the system. The change in fluorescence signal was directly proportional to the PKA concentration in the range 0–1.8 U/ml with a detection limit of 0.04 U/ml. These results suggest that PKA activity can be effectively measured using the developed PKA biosensor. Moreover, the fluorescence biosensor was successfully used in the investigation of PKA in spiked human embryonic kidney (HEK) 293 cells lysates, indicating its potential applications in protein kinase-related biochemical fundamental research.

KEYWORDS
biosensor, carboxylic carbon nanoparticles, fluorescence, peptide, protein kinase A

1 | INTRODUCTION

Protein kinase phosphorylation plays a major regulatory role in the immune response, signal transduction, metabolism, and other important cellular activities.[1,2] Protein kinase A (PKA) is a type of protein that catalyzes the transfer of γ-phosphoryl from adenosine-5′-triphosphate (ATP) to specific amino acids.[3,4] Additionally, it plays a crucial role in the transduction of intracellular signals and regulation of cellular functions including cell growth, cell signal communications, and survival differentiation.[5,6] Abnormal expression of protein kinase has been implicated in some diseases such as diabetes, Alzheimer's disease, and cancers.[7–10] So, the establishment of a simple and sensitive approach for monitoring the PKA activity is of great significance for the diagnosis and treatment of kinase-related diseases.

At this time, the two methods used in detecting protein kinase activity are based on radiometric assays using radioactive ATP with γ-^{32}P and immunoassays using a phosphospecific antibody.[11–13] The above assays are frequently used to analyze the PKA activity in most laboratories, but they have some drawbacks. Radioactive methods pose high risks because of the involvement of harmful radioactive substances. Immunoassays require sophisticated processes and high cost. To overcome these problems, various techniques including fluorescence-based methods,[14–18] colorimetry,[19–21] electrochemistry,[22–24] and mass spectrometry[25] have been established for the assay of PKA activity. These approaches are novel and of great potential to be used in detecting protein kinase activity. However, some of these approaches exhibit either moderate sensitivity or low efficiency. For instance, Yang and colleagues have proposed an interesting and novel strategy for detecting protein kinase activity using Zr^{4+}-functionalized magnetic beads and a commercial personal glucose meter.[26] Song and colleagues reported a spectroscopic probe using peptide–gold nanoclusters for detecting the kinase. Although

this method has a low detection limit, the method is time consuming and high cost.[16] Therefore, it is necessary to construct inexpensive, specific, and sensitive methods for detecting kinase activity.

In recent years, to develop a novel technique for life sciences and biotechnology, significant numbers of nanomaterials with unique chemical and physical properties were combined with specific recognition elements.[27–29] Gold nanoparticles, carbon nanomaterials, and silica nanoparticles have emerged. Additionally, they have widespread applications, particularly in drug delivery, therapy, and diagnostics *in vivo* and *in vitro*.[30–32] In particular, carbon nanomaterials have gained significant attention for successful application in various biomedical and bioanalytical fields. Therefore, carbon nanoparticles (CNPs) have been proved to have many excellent properties, especially the nature of its quenching, which has been imaginatively used to build various new-style tools in bioanalysis, such as for biosensors. Li and colleagues demonstrated that the single-stranded probe can be adsorbed onto the surface of the CNPs via π–π interaction, resulting in quenching of the system via fluorescence resonance energy transfer (FRET).[33] Lin and colleagues reported that the fluorescence of the dye-labelled aptamer can be effectively quenched by the CNPs, therefore serving as a promising sensing platform for the detection of biomolecules such as ATP and kanamycin.[34] Liu and colleagues designed a rapid and simple means for detecting thrombin based on the CNPs with single-stranded DNA.[35] Nevertheless, there have been relatively few studies on CNPs compared with other carbon materials. To date, there has been no study on designing this type of CNP–peptide fluorescent sensors for monitoring PKA, therefore it is encouraged to develop CNP–peptide fluorescent sensors for PKA activity.

Here, for the first time, a facile method for PKA assay was constructed based on CNPs (Scheme 1). A purpose-designed peptide (CGGLSARRL) was synthesized. With the presence of ATP, PKA can phosphorylate the designed substrate at the serine position.[4,5] The oxidized CNPs with the groups COO^- and OH^- are used as a fluorescence sensing platform. We predicted that the interaction force between CNPs and the peptide would alter the fluorescence intensity of the sensor after phosphorylation. First, a carboxyfluorescein (FAM)-labelled peptide with the core substrate (CGGLSARRL) was designed. Next, the FAM-labelled peptide containing two positively charged Arg residues (RR) was mixed with CNPs to form the biosensor between them.[33,35] As a consequence, the fluorescence of the system was quenched. Specifically, upon reaction with ATP and PKA, the peptide was phosphorylated by PKA, and a phosphate group containing two negative charges was added to the peptide, resulting in zero charge of the peptide and a weak interaction between them. Therefore, the fluorescence recovery of the system occurred due to the disruption of FRET. This approach provides a neoteric readout for PKA.

2 | EXPERIMENTAL

2.1 | Apparatus

Fluorescence spectra were measured using an F2500 fluorescence spectrophotometer (Hitachi Ltd, Tokyo). The ζ-potential was measured on a Malvern nano ZS instrument (Malvern, the UK). Scanning electron microscopy (SEM) analysis was done using a Gemini SEM 300 (ZEISS, Germany). Transmission electron microscopy (TEM) images were taken using a JEM-1011 instrument. Fourier transform infrared (FT-IR) spectra were recorded on a Nicolet iS50 spectrometer (Thermo Fisher Scientific, USA). The analysis of PKA was performed in a Thermomixer C (Eppendorf, Germany). An AHI-98128 pH meter (Hanna Instruments Inc., Woonsocket, USA) was used for pH measurements.

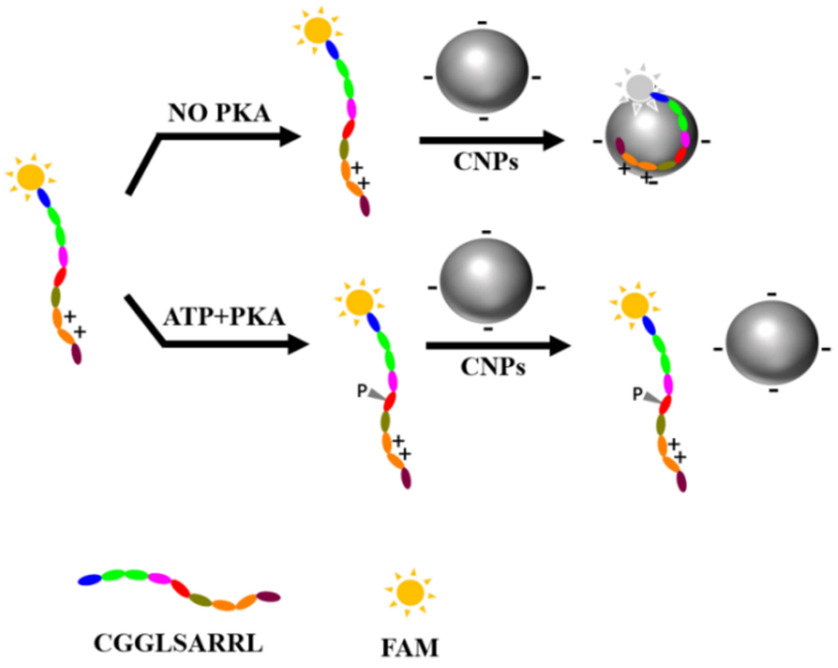

SCHEME 1 Schematic illustration of the carboxylic CNP–peptide fluorescent biosensor for monitoring protein kinase activity

2.2 | Materials and reagents

Protein kinase A (PKA), H-89 dihydrochloride hydrate, dithiothreitol (DTT), fetal bovine serum (FBS), ATP disodium salt hydrate, phosphorylase kinase (PhK) and protein kinase G 1β human (PKG1β) were obtained from Sigma-Aldrich. *N*,*N*-Dimethylformamide (DMF), HCl, 98% nitric acid, NaCl, and EDTA were obtained from Beijing Chemicals, Ltd. Bovine serum albumin (BSA), thrombin, trypsin, carboxylesterase (CarE), glucose oxidase (GOD), urease, and glycerol were obtained from J&K Chemical. Human PKCα recombinant (PKCα) and human casein kinase 2α protein (CK2α) were obtained from Chemegen and Bio-Tech Pioneer. Tris(hydroxymethyl)aminomethane (Tris) was obtained from Shanghai Aladdin Reagent Co., Ltd. A Tris–HCl buffer (20 mM, 50 mM NaCl, 10 mM $MgCl_2$, pH 7.5) was prepared and used for subsequent experiments. The PKA solution was prepared using the Tris–HCl buffer (20 mM), containing 50 mM NaCl, 1 mM EDTA, 2 mM DTT, 50% glycerol, and then divided into suitable amounts for follow-up experiments. The FAM-labelled peptides (purchased from Shanghai Sangon Biotech Co., Ltd) had the following sequences: FAM-CGGLSARRL for S-peptide and FAM-CGGLpSARRL for phosphorylated (P)-peptide. All other chemical reagents were analytically pure. Milli-Q water was used in all the experiments.

2.3 | Synthesis of carboxylic group-functionalized CNPs

Dry candle soot was obtained from the combustion of candles.[36] Next, 4.0 mg of dry candle soot was dissolved in DMF (2 ml) and nitric acid (98%, 2 ml). The oxidized CNPs were obtained after refluxing at 140°C for 12 h. After being cooled under ambient conditions, the reaction solution was centrifuged, and the upper liquid layer was removed. The sediment was washed several times using ultrapure water until neutral. The carboxylic group-functionalized CNPs were obtained after being dried at 60°C for 12 h. To form a homogeneous black solution, the CNPs were dispersed in water and then sonicated for 10 min to form a stable solution with a concentration of 0.5 mg/ml.

2.4 | General procedure for detecting PKA activity and its inhibitor

All stock solutions of the peptide with a concentration of 10 μM were obtained by dissolving the corresponding quality of peptide into a buffer solution. The solution of ATP with a concentration of 1.0 mM was obtained after dissolving a certain quality in Tris–HCl buffer.

To detect PKA activity, 10 μl of peptide solution (10 μM), 40 μl of ATP solution (1.0 mM), and 20 μl PKA solutions with different concentrations were mixed with 600 μl Tris–HCl and then incubated at 37°C for 1 h. Next, 60 μl CNPs, 270 μl Tris–HCl and the above reaction solution were mixed to obtain the final measured volume of 1 ml. The final PKA concentrations were 0, 0.4, 0.8, 1.0, 1.20, 1.40, 1.60, 1.80, 2.0, 2.4, and 2.8 U/ml. After 10 min, the fluorescence intensity/spectrum of each sample was monitored at $\lambda_{ex/em} = 470/520$ nm.

The procedure for the PKA inhibitor assay was similar to the procedure described above, except that the inhibitors and PKA were mixed into the reaction solution.

2.5 | Detection of PKA activity in HEK 293 cell lysates

Normal human embryonic kidney (HEK) 293 cells (1×10^6 cells) were cultured in Dulbecco's modified Eagle's medium supplemented with 10% FBS and then incubated at 37°C under a humidified atmosphere containing 5% CO_2 for 24 h. To remove the supernatant, the cultured cells were centrifuged after being incubated in serum-free medium for 4 h and then lysed using an ultrasonic liquid processor for 5 min. The cell lysates were centrifuged for 30 min at 20,000 rpm at 4°C. The extracted supernatants were stored at −20°C for subsequent experiments. To demonstrate the practical application of the biosensor, solutions of three different PKA concentrations were spiked into the cell lysates. Thereafter, the reaction system with equal volumes of the prepared cell lysate samples was used to detect the PKA activity. For comparison, the cell lysate sample with no spiked PKA was measured using similar conditions.

3 | RESULTS AND DISCUSSION

3.1 | The characterization of carboxylic group-functionalized CNPs

To increase their water solubility, the candle soot obtained from combustion of candles was first treated with nitric acid to obtain the oxidized CNPs with the groups COO^- and OH^-. The morphological characterization of the oxidized CNPs was carried out via TEM and SEM. The TEM and SEM images showed that the oxidized CNPs had good dispersibility (Figure 1). From the TEM images, it can be observed that the approximate size distributions of the oxidized CNPs were ~30–40 nm, no more than 70 nm. Figure 1D shows the FT-IR spectra of both candle soot and the carboxylic group-functionalized CNPs. The peaks at ~3423 and 1109 cm^{-1} in both spectra were due to the characteristic absorption bands of the –OH stretching vibration mode. The characteristic absorption band of $-CH_2-$ stretching at 2921–2852 cm^{-1} was also observed, and the peak at 1384 cm^{-1} could be attributed to the C–H stretching mode. For the carboxylic group-functionalized CNPs, the peaks at 1630 cm^{-1} could be evidently attributed to the C=O stretching mode, and they indicated the generation of the COOH groups. These observations confirmed that the carboxylic group-functionalized CNPs function with the moieties of hydroxyl and carboxylic/carbonyl. The FT-IR and TEM data showed that COOH groups could be formed on CNPs by acid treatment. The zeta potential of the carboxylic group-functionalized CNPs was

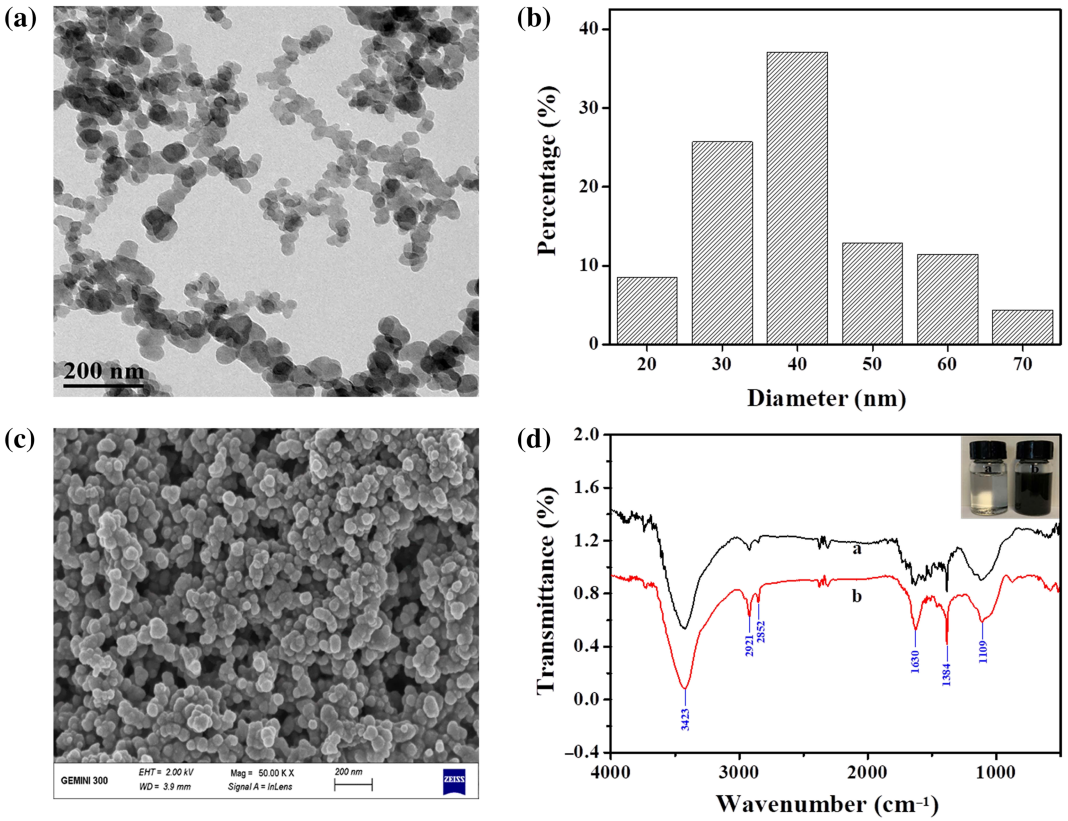

FIGURE 1 (a) TEM image of CNPs. (b) Size distribution histograms of the CNPs. (c) SEM image of the CNPs. (d) FT-IR spectra of (curve a) candle soot and (curve b) the carboxylic group-functionalized CNPs

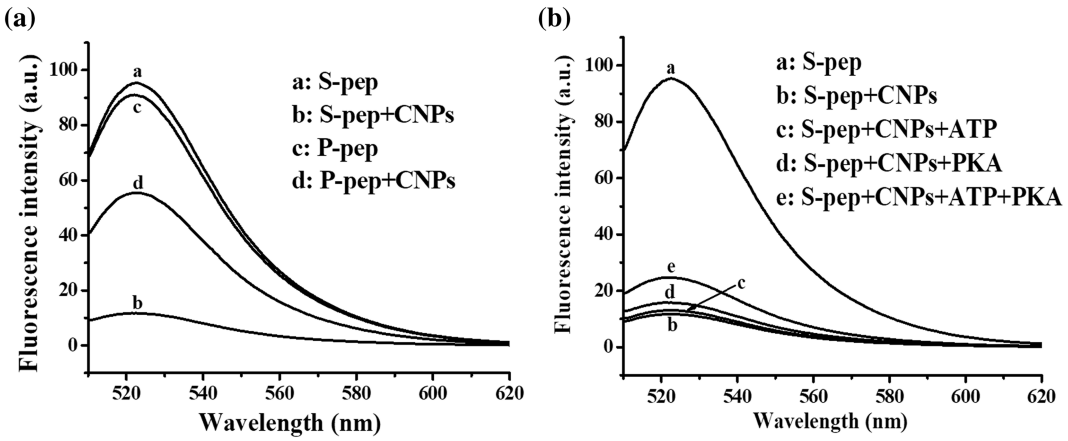

FIGURE 2 (a) Fluorescence spectra of different reaction systems: (curve a) FAM-labelled S-peptide (100 nM); (curve b) system (curve a) + CNPs (30 μg/ml); (curve c) FAM-labelled P-peptide (100 nM); (curve d) system (curve c) + CNPs (30 μg/ml). (b) Fluorescence spectra of different reaction systems: (curve a) the FAM-labelled S-peptide (100 nM); (curve b) system (curve a) + CNPs (30 μg/ml); (curve c) system (curve b) + ATP (40 μM); (curve d) system (curve b) + PKA (1.0 U/ml); (curve e) system (curve b) + ATP (40 μM) + PKA (1.0 U/ml)

approximately −35.4 ± 5.42 mV, therefore indicating that the carboxylic group-functionalized CNPs had a negatively charged surface, which may be because of the presence of COOH groups. Therefore, the zeta potential could have enormous influence on ion stability through the electrostatic repulsion between particles, which contributed to the good water solubility of CNPs.

3.2 | Feasibility analysis of the method

To verify the feasibility of the CNP-based fluorescence design for monitoring the PKA activity clearly, the results were analyzed. It can be observed in Figure 2(a) that the specifically designed S-peptide and P-peptide exhibited strong fluorescence centred at ~522 nm

(compare curves a and c in Figure 2a). The fluorescence intensity of the system decreased (curve b in Figure 2a) when the CNPs solution was added to the S-peptide. However, the P-peptide at a similar concentration showed only a small influence on the signal intensity of the system (curve d in Figure 2a). Moreover, after separately mixing with ATP or PKA, the signal intensity of the CNPs/S-peptide system did not change significantly (curves c and d in Figure 2b). Upon reacting with PKA and ATP, the S-peptide in the system was phosphorylated by the PKA, and phosphopeptides were removed from the CNP surface, resulting in enhancement of the signal intensity enhancement (curve e in Figure 2b). The high discriminative ability of the designed sensor towards S-peptide and P-peptide is a reliable basis for monitoring PKA activity, which can be reflected easily and proportionally by the change in fluorescence intensity.

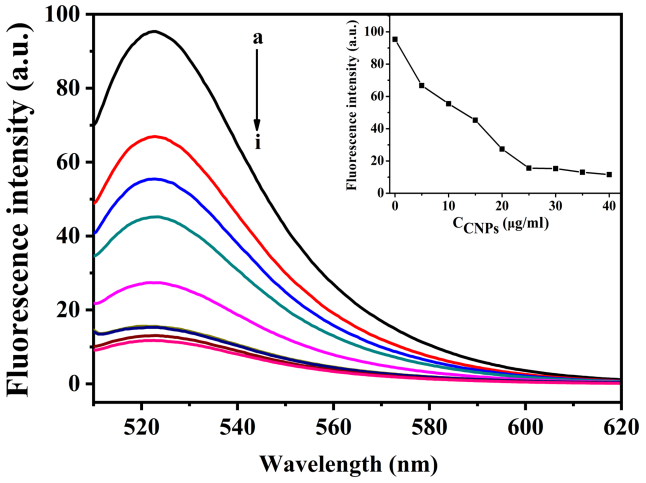

FIGURE 3 Fluorescence spectra of the FAM-labelled peptide (100 nM) in Tris–HCl buffer in the presence of various concentrations of CNPs: (1) 0.0, (2) 5.0, (3) 10.0, (4) 15.0, (5) 20.0, (6) 25.0, (7) 30.0, (8) 35.0, and (9) 40.0 μg/ml. Inset: Fluorescence intensity versus CNPs concentration

3.3 | Optimization of experimental conditions

To construct the CNP–peptide fluorescent sensor, the concentration of CNPs was first optimized for the FAM-labelled peptide. As is seen in Figure 3, the peptide solution without CNPs showed a strong signal intensity. The fluorescence gradually decreased with the increase in the amount of CNPs. As shown in the inset of Figure 3, with 25 μg/ml CNPs, the signal quenching of the system was 85%, implying that strong interaction between CNPs and the peptide. This phenomenon can be attributed to the efficient electron transfer from CNPs to the FAM-labelled peptide.[14] In addition, the Stern–Volmer plot of the CNPs showed a downward bending and indicated the formation of a static quenching complex between them (the inset in Figure 3). As shown in Figure 4(a), kinetic experiments on the CNP–peptide biosensor were conducted. After adding the CNPs to the FAM-peptide solution, the signal intensity of the system decreased sharply and reached equilibrium, revealing that the reaction between the peptide and CNPs was very fast. In our research, the sensor was fabricated by the mixture of the peptide solution (100 nM) with CNPs (30 μg/ml) in 20 mM Tris–HCl. Moreover, the concentration of ATP played an important role in the detection of PKA. As illustrated in Figure 4(b), the signal intensity of the sensor achieved equilibrium when the amount of ATP was 40 μM. Therefore, a final concentration of 40 μM was used for the subsequent experiments.

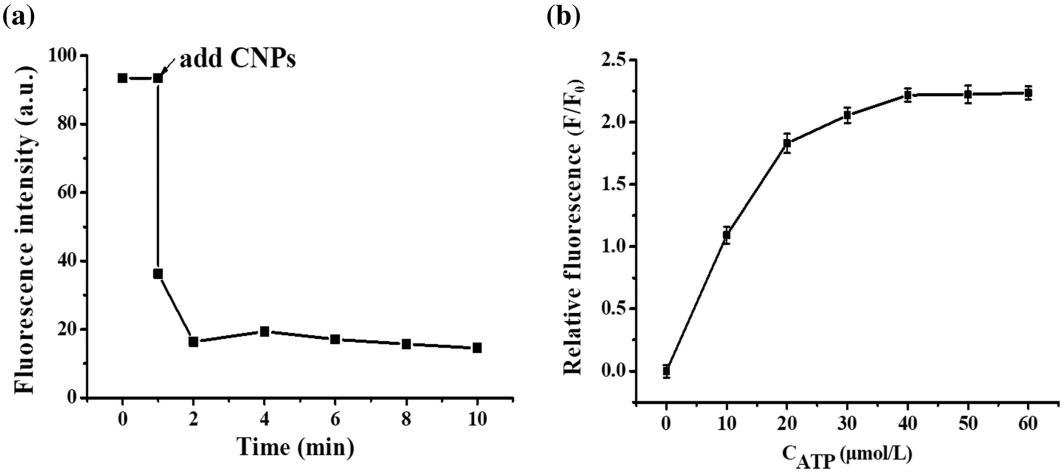

FIGURE 4 (a) Fluorescence quenching of FAM-labelled peptide (100 M) by CNPs (30 μg/ml) in Tris–HCl (7.5) as a function of time. (b) Effect of ATP concentration on the fluorescence intensity ratio of peptide/CNPs/PKA/ATP system. F_0 is the fluorescence intensity of peptide/CNPs/PKA/ATP system in the absence of ATP; F is the fluorescence intensity of peptide/CNPs/PKA/ATP system in the presence of ATP. CNPs: 30 μg/ml; peptide: 100 nM; PKA: 1.0 U/ml

3.4 | Detection of the PKA activity and inhibitor

To verify the response of the constructed biosensor to PKA, the CNP–peptide sensor was treated with an ATP at a fixed concentration and PKA at different concentrations in 20 mM Tris–HCl at 37°C for 1 h and the fluorescence spectra of each solution was subsequently recorded. The signal intensity of the sensor increased with the increasing concentration from 0 U/ml to 1.8 U/ml (Figure 5a). This indicated the formation of a phosphorylated peptide with a weaker electrostatic interaction between the FAM and CNPs. From Figure 5(b), it can be observed that the fluorescence intensity is directly proportional to the PKA concentration ranging from 0 to 1.8 U/ml, yielding a good linear equation: $F/F_0 = 0.6329\ [PKA]\ (U/ml) + 1.0387$ ($R^2 = 0.9913$). The detection limit (3S/m, where S is the standard deviation of blank measurements, $n = 11$, and m is the slope of the linear equation)[37,38] was determined to be 0.04 U/ml. This numerical value is lower than that in the fluorescence method based on graphene oxide.[4] Moreover, the FAM-labelled peptide/ATP (control experiment) system without CNPs did not exhibit any major change in signal intensity when the equivalent concentration of PKA was added (Figure 5b). This shows that the CNPs are of great concern to the construction of the sensor. Additionally, the fluorescence change of the sensor as a function of time was explored. As is seen in Figure 6, with PKA at a high concentration in the system, the result showed that strong intensity can occur, and the signal intensity increased to a plateau in ~1 h. Therefore, the reaction time in all the experiments was 1 h.

To prove that the fluorescence enhancement was attributed to PKA, the effect of H-89 (a potential and cell-permeable inhibitor of PKA) on the activity of PKA was investigated. First, the peptide/ATP/PKA/H-89 system was mixed and pretreated at 37°C for 1 h, and then CNPs were added to the pretreated solution. As observed in Figure 7, the fluorescence intensity of the sensor hardly changed in the presence or absence of H-89 (compare curves a and c). However, the signal intensity of the reaction system with H-89 decreased significantly (please refer to curves b and d). This displays that the enhanced signal intensity was evidently caused by the PKA activity. Therefore, the PKA activity could be significantly inhibited by H-89, revealing that our established sensor can be applied to the discovery for PKA inhibitors.

3.5 | Selectivity of the detection system

To explore the specificity of our proposed sensor, thrombin, trypsin, carboxylesterase (CarE), glucose oxidase (GOD), urease, phosphorylase kinase (PhK), protein kinase G 1β human (PKG1β), human PKCα recombinant (PKCα), human casein kinase 2α protein (CK2α) and BSA, were studied in parallel under optimal experimental conditions. The

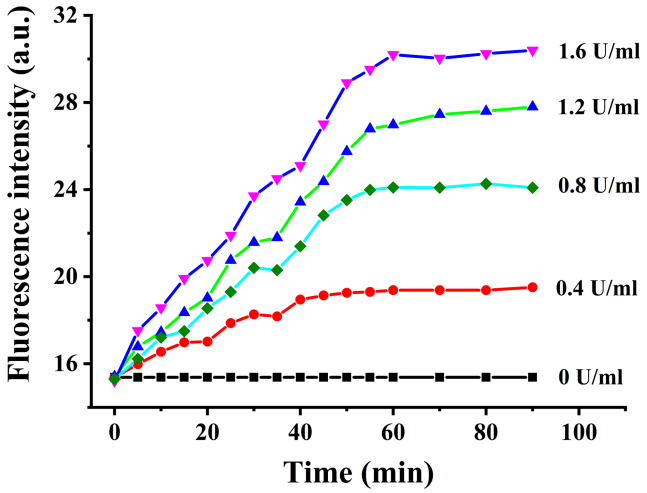

FIGURE 6 Time-resolved measurements of PKA activity with various concentrations of PKA

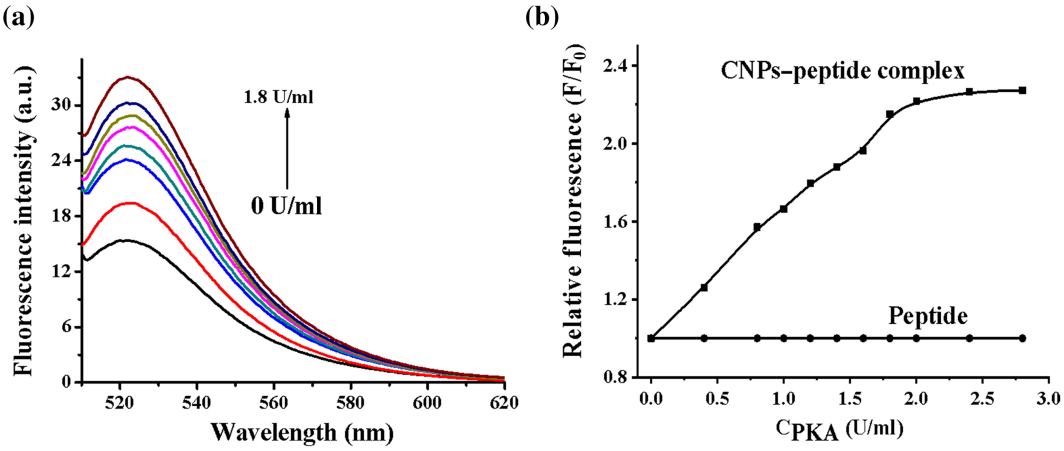

FIGURE 5 (a) Fluorescence response of the sensor to PKA at various concentrations (0, 0.4, 0.8, 1.0, 1.20, 1.40, 1.60, and 1.80 U/ml). (b) Relative fluorescence changes of the peptide/ATP and the CNPs/peptide/ATP complex at various PKA concentrations (0, 0.4, 0.8, 1.0, 1.20, 1.40, 1.60, 1.80, 2.0, 2.4, and 2.8 U/ml) at 522 nm

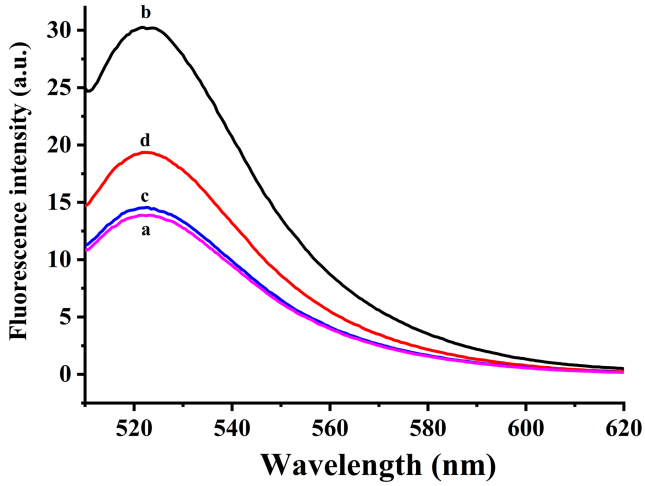

FIGURE 7 Fluorescence spectra of different reaction systems: (curve a) CNPs/peptide/ATP complex in Tris–HCl with a pH of 7.5 (control); (curve b) system (curve a) + 1.6 U/ml PKA; (curve c) system (curve a) + H-89 (1 mM); (curve d) system (curve b) + H-89 (1 mM)

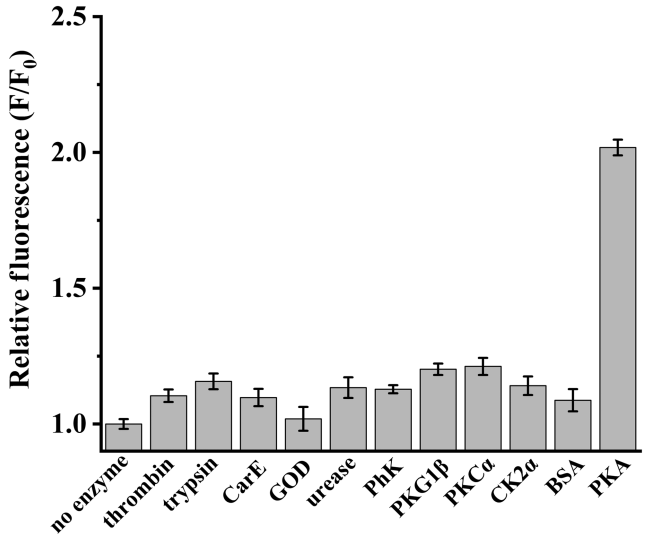

FIGURE 8 Fluorescence responses of the system to different enzymes: (a) no enzyme, (b) 4.0 U/ml thrombin, (c) 4.0 U/ml trypsin, (d) 4.0 U/ml CarE, (e) 4.0 U/ml GOD, (f) 4.0 U/ml urease, (g) 4.0 U/ml PhK, (h) 100 nM PKG1β, (i) 100 nM PKCα, (j) 100 nM CK2α, (k) 100 nM BSA, and (l) 1.6 U/ml PKA

results showed that the reaction system exhibited significantly higher fluorescence recovery by PKA (Figure 8). The results clearly showed that our designed method is selective and specific for detecting PKA.

3.6 | Detection of PKA activity in HEK 293 cell lysates

PKA plays a crucial part in cell signalling, the immune response and cellular regulation. Moreover, the measurement of PKA activity in cell lysates is of great importance in clinical studies. To prove the usefulness of the established method, HEK 293 cells were selected as the cell model for PKA analysis. In particular, HEK 293 cell lysates with different concentrations of PKA were measured using our established methods. As shown in Table 1, the test results were satisfactory. The recoveries of PKA in the spiked cell lysate samples detected by our proposed method ranged from 98.3 to 107.5%, and the relative errors were less than 6%, indicating that our proposed approach could be successfully applied in clinical studies.

4 | CONCLUSION

We have constructed a simple platform for detecting PKA based on CNPs. The method is simple and specific because the changes in fluorescence signal can only be initiated by the formation of phosphorylated peptide with the introduction of ATP and PKA. Therefore, compared with existing fluorescence kinase assays, the established method is able to detect PKA without the involvement of sophisticated processes. Notably, this is the first example of a CNP-based biosensing method for PKA. Moreover, the preliminary application of the proposed approach in the investigation of HEK 293 cell lysates provides a promising means for fundamental research on PKA-related biochemistry and PKA-targeted drug screening.

ACKNOWLEDGEMENTS

We thank the financial support from the National Natural Science Foundation of China (82003925), the China Postdoctoral Science Foundation (2019 M662089) and the Science and Technology Innovation Project of Colleges and Universities in Shanxi Province (2020L0413).

TABLE 1 Determination of PKA spiked into HEK 293 cell lysates

Sample	PKA added (U/ml)	PKA detected[a] (U/ml)	Recovery(%)[a]
HEK 293	0	<0.04 (detection limit)	—
	0.40	0.43 ± 0.01	107.5 ± 2.5
	0.80	0.82 ± 0.04	102.5 ± 5.0
	1.20	1.18 ± 0.05	98.3 ± 4.2

[a]Mean of three determinations ± standard deviation.

ORCID

Tingting Feng https://orcid.org/0000-0002-8221-0989

REFERENCES

[1] Y. L. Zhou, H. S. Yin, X. Li, Z. Li, S. Y. Ai, H. Lin, *Biosens. Bioelectron.* **2016**, *86*, 508.
[2] D. M. Rothman, M. D. Shults, B. Imperiali, *Trends Cell Biol.* **2005**, *15*, 502.
[3] R. S. Agnes, F. Jernigan, J. R. Shell, V. Sharma, D. S. Lawrence, *J. Am. Chem. Soc.* **2010**, *132*, 6075.
[4] Q. Liu, N. Li, M. K. Wang, L. Wang, X. G. Su, *Anal. Chim. Acta* **2018**, *1013*, 71.
[5] Y. H. Xu, W. Shi, X. Y. He, X. F. Wu, X. H. Li, H. M. Ma, *Anal. Chem.* **2017**, *89*, 10980.
[6] C. Yin, M. Wang, C. Y. Lei, Z. Wang, P. Li, Y. Li, W. Li, Y. Huang, Z. Nie, S. Z. Yao, *Anal. Chem.* **2015**, *87*, 6311.
[7] M. M. Soundarapandian, C. A. Juliana, J. H. Chai, P. A. Haslett, K. Fitzgerald, D. D. De León, *PLoS ONE* **2020**, *15*, e0236892.
[8] H. J. Ko, S. J. Chiou, Y. H. Wong, Y. H. Wang, Y. L. Lai, C. H. Chou, C. Wang, J. K. Loh, A. S. Lieu, J. T. Cheng, Y. T. Lin, P. J. Lu, M. J. Fann, C. Y. Huang, Y. R. Hong, *J. Clin. Med.* **2019**, *8*, 1751.
[9] G. D. B. Machado, B. S. de Freitas, L. Z. Florian, R. T. Monteiro, H. Gus, N. Schröder, *J. Neuroendocrinol.* **2019**, *31*, e12780.
[10] S. Zada, J. S. Hwang, M. Ahmed, T. H. Lai, T. M. Pham, D. H. Kim, D. R. Kim, *Oncol. Rep.* **2019**, *42*, 1621.
[11] J. E. Hutti, E. T. Jarrell, J. D. Chang, D. W. Abbott, P. Storz, A. Toker, L. C. Cantley, B. E. Turk, *Nat. Methods* **2004**, *1*, 27.
[12] K. Farley, H. Mett, E. McGlynn, B. Murray, N. B. Lydon, *Anal. Biochem.* **1992**, *203*, 151.
[13] B. Schraag, G. E. Staal, S. S. Adriaansen-Slot, M. Salden, G. Rijksen, *Anal. Biochem.* **1993**, *211*, 233.
[14] L. Wang, X. Yan, X. G. Su, *Anal. Chim. Acta* **2016**, *935*, 224.
[15] S. Y. Tang, Y. F. Hu, Q. P. Shen, H. T. Fang, W. Li, Z. Nie, S. Z. Yao, *Analyst* **2014**, *139*, 4710.
[16] W. Song, R. P. Liang, Y. Wang, L. Zhang, J. D. Qiu, *Chem. Commun.* **2015**, *51*, 10006.
[17] X. B. Zhang, C. H. Liu, H. H. Wang, H. Wang, Z. P. Li, *Angew. Chem. Int. Ed.* **2015**, *54*, 15186.
[18] F. Ma, Y. Li, B. Tang, C. Y. Zhang, *Acc. Chem. Res.* **2016**, *49*, 1722.
[19] S. J. Sun, H. X. Shen, C. H. Liu, Z. P. Li, *Analyst* **2015**, *140*, 5685.
[20] Z. X. Wang, R. Lévy, D. G. Fernig, M. Brust, *J. Am. Chem. Soc.* **2006**, *128*, 2214.
[21] J. Zhou, X. H. Xu, X. L. Liu, H. Li, Z. Nie, M. Qing, Y. Huang, S. Z. Yao, *Biosens. Bioelectron.* **2014**, *53*, 295.
[22] J. Q. Liu, X. X. He, K. M. Wang, D. G. He, Y. H. Wang, Y. F. Mao, H. Shi, L. Wen, *Biosens. Bioelectron.* **2015**, *70*, 54.
[23] B. Y. Li, X. H. Shi, W. Gu, K. Zhao, N. N. Chen, Y. Z. Xian, *Analyst* **2013**, *138*, 7212.
[24] H. F. Zhao, R. P. Liang, J. W. Wang, J. D. Qiu, *Chem. Commun.* **2015**, *51*, 12669.
[25] Y. P. Kim, E. Oh, Y. H. Oh, D. W. Moon, T. G. Lee, H. S. Kim, *Angew. Chem. Int. Ed.* **2007**, *46*, 6816.
[26] W. X. Yang, X. H. Lu, Y. C. Wang, S. J. Sun, C. H. Liu, Z. P. Li, *Sens. Actuators B* **2015**, *210*, 508.
[27] X. L. Li, Y. F. Bai, F. Feng, Z. J. Zhang, *Luminescence* **2017**, *32*, 730.
[28] J. Kubackova, J. Zbytovska, O. Holas, *Eur. J. Pharm. Sci.* **2020**, *142*, 105139.
[29] L. Yan, F. Zhao, J. Wang, Y. Zu, Z. J. Gu, Y. L. Zhao, *Adv. Mater.* **2019**, *31*, e1805391.
[30] Z. Saberi, B. Rezaei, T. Khayamian, *Luminescence* **2018**, *33*, 640.
[31] H. J. Song, C. F. Wang, H. P. Zhang, L. Yao, J. J. Zhang, R. X. Gao, X. S. Tang, T. Chong, W. P. Liu, Y. H. Tang, *Colloids Surf. B. Biointerfaces* **2019**, *182*, 110375.
[32] Z. Y. Wang, H. Liao, H. Wu, B. B. Wang, H. D. Zhao, M. Q. Tan, *Anal. Methods* **2015**, *7*, 8911.
[33] H. L. Li, Y. W. Zhang, L. Wang, J. Q. Tian, X. P. Sun, *Chem. Commun.* **2011**, *47*, 961.
[34] X. Y. Lin, L. Cui, Y. S. Huang, Y. Lin, Y. Xie, Z. Zhu, B. C. Yin, X. Chen, C. Y. James Yang, *Chem. Commun.* **2014**, *50*, 7646.
[35] J. H. Liu, J. S. Li, Y. Jiang, S. Yang, W. H. Tan, R. H. Yang, *Chem. Commun.* **2011**, *47*, 11321.
[36] H. P. Liu, T. Ye, C. D. Mao, *Angew. Chem. Int. Ed.* **2007**, *46*, 6473.
[37] T. T. Feng, H. M. Ma, *Analyst* **2013**, *138*, 2438.
[38] D. Feng, Y. Y. Zhang, T. T. Feng, W. Shi, X. H. Li, H. M. Ma, *Chem. Commun.* **2011**, *47*, 10680.

How to cite this article: T. Feng, S. Yan, Z. Wang, X. Fan, *Luminescence* **2022**, *37*(6), 922. https://doi.org/10.1002/bio.4237